An improved contact model considered the effect of boundary lubrication regime on piston ring-liner contact for the two-stroke marine engines from the perspective of the Stribeck curve

Journal:	*Part C: Journal of Mechanical Engineering Science*
Manuscript ID	JMES-21-0636.R1
Manuscript Type:	Original Research Article
Date Submitted by the Author:	24-May-2021
Complete List of Authors:	Xiuyi, Lyu; Harbin Engineering University; University of Leeds School of Mechanical Engineering Jiao, Bowen; Haerbin Engineering University, College of Power and Energy Engineering Wang, Yuechang; University of Leeds School of Mechanical Engineering Azam, Abdullah; University of Leeds School of Mechanical Engineering Lu, Xiqun; Harbin Engineering University, College of Power and Energy Engineering Zou, Dequan; Washington University in St Louis Ma, Xuan; Harbin Engineering University, College of Power and Energy Engineering Neville, Anne; University of Leeds School of Mechanical Engineering
Keywords:	Piston ring cylinder liner system, Statistical lubrication model, Boundary lubrication regime, Marine Engineering, Two-Stroke Engine
Abstract:	Due to the global drive towards low emission ships and stricter environmental regulations, two-stroke engines have attracted more attention since their highly effective and economical. It has been suggested that most of the energy loss in marine engines is caused by the friction within the piston ring-cylinder liner (PRCL) system. The prediction of lubrication performance is required to be the basement of friction optimization. In engineering applications, statistical models have become a practical choice in engine development due to the advantages of fast, efficient, and macroscopic fault location. Boundary lubrication exists in the PRCL system of two-stroke marine engines because of the harsher load, lower speed, and larger structure. It has been proposed that there would be tribofilm under boundary lubrication which has a significant influence on the contact. However, the growth of tribofilm is directly related to the asperities contact pressure of surfaces. Therefore, whether the contact pressure calculation in existing statistical modes could be adapted to boundary lubrication is an issue worthy of attention. This study introduces the calculation of asperities contact pressure under boundary lubrication, which Wen proposed, into the classic Greenwood-Williamson model, the problem that the original model cannot reflect the boundary lubrication regime in the form of the Stribeck curve is improved. Furthermore, the boundary lubrication regime does exist indeed near the top dead center of two-stroke engines. Finally, the results are compared before and after modifying the model to verify this study's practicability. This study improves the defects of the statistical model of two-stroke engines in the boundary lubrication phase. It provides preconditions for the subsequent tribofilm research under the

	PRCL statistical model.

An improved contact model considered the effect of boundary lubrication regime on piston ring-liner contact for the two-stroke marine engines from the perspective of the Stribeck curve

Lyu Xiuyi[1,2], Bowen Jiao[1], Yuechang Wang[2], Abdullah Azam[2], Xiqun Lu[1], Dequan Zou[1,3], Xuan Ma[1*], Anne Neville[2]

[1] Harbin Engineering University, Harbin, Heilongjiang, China

[2] Mechanical engineering, University of Leeds, LS29JT, UK

[3] Washington University in St. Louis, St. Louis, MO, USA

*Corresponding author Email: maxuan@hrbeu.edu.cn, Tel: +86 0451-82588833-321, Fax: +86 82588833-311

Abstract: The prediction of lubrication performance is required to be the basement of friction optimization for marine engines. This paper simulates the lubrication performance of marine engines based on statistical models which have the advantages of fast, efficient, and macroscopic fault location. Boundary lubrication exists in the piston ring-cylinder liner (PRCL) of two-stroke marine engines because of the harsher load, lower speed, and larger structure. It has been proposed that there would be tribofilm under boundary lubrication which has a significant influence on the contact. To understand the boundary lubrication, it is necessary to study the lubrication regime transition. In this paper, firstly, the coefficient of friction curve combined with the thickness ratio embodies the lubrication regime transition process of two-stroke engines under work conditions. However, the phenomenon that the coefficients under boundary lubrication are smaller than that of other regimes shows the non-objectivity of this curve. Therefore, the Stribeck curve is introduced for objectively evaluating the transition. Then, the calculation of asperities contact pressure under boundary lubrication, which Wen proposed, is introduced into the classic Greenwood-Williamson model, the problem that the original model cannot reflect the boundary lubrication regime in the form of the Stribeck curve is improved. Finally, the results are compared before and

after modifying the model to verify this study's practicability. It provides more precise asperities contact pressure for the tribofilm growth calculation from the perspective of the Stribeck curve under the PRCL statistical model in future work.

Keywords: Piston ring cylinder liner system; Statistical lubrication model; Boundary lubrication regime; Marin engineering; Two-stroke engines.

1. Introduction

The advantages of reliable power output, high engine efficiency, and low operating and maintenance costs of two-stroke engines make them the first choice for large-scale ocean freighters. Meanwhile, the deterioration of various friction pairs' operating conditions is caused by the continuous pursuit of high-power density from the low-speed marine diesel engines. Furthermore, it has been proposed that most of the mechanical power loss in internal combustion engines (ICEs) is related to the piston ring-cylinder (PRCL) system[1,2]. Therefore, a precise prediction of lubrication performance in the PRCL system is required to reduce emissions, increase service life, and improve the reliability of ICEs.

At present, the tribology numerical models are mainly divided into statistical models and deterministic models. The deterministic model needs all the details of the surface [3]. For the studies of a two-stroke marine engine with a large cylinder diameter and a complex surface structure, the use of a deterministic model is a tedious and labor-intensive project. Statistical models have become a practical choice in engine development due to the advantages of fast, efficient, and macroscopic fault location. An early study of modeling lubrication of the PRCL system was proposed by Rohde et al.[4], which is combing the average Reynolds equation with the asperity contact model developed by Greenwood and Tripp[5], under the boundary condition obtained by Patir and Cheng[6]. Greenwood-Tripp model is extensively used to calculate microcontact and pressures that arise when two rough surfaces approach each other. Some engineering surfaces, and certainly those in engines have the non-Gaussian distribution

of asperity heights. Leighton[35] dealt with practical engineering surfaces from laboratory-based testing using a sliding tribometer to accelerated fired engine testing for high-performance applications of cross-hatched honed cylinder liners. This work helps understand how to deal with rough non-Gaussian distribution surfaces. J.X. Pei[36] investigated the influence of non-Gaussian rough surfaces on the mixed EHL of line contact, which could be further used for evaluating the state and reliability of lubrication. For simplification, Eduardo[7] focused on the Greenwood-Williamson model and applied it to the PRCL system, which could be directly applied to rough engine surfaces. A hydrodynamic lubrication model was introduced by Dowson et al.[8] for the description of oil film thickness and viscous friction in the PRCL contacts. By improving the model of Dowson, Jeng[1] relaxed the assumption of flow factors to develop a one-dimensional model for oil film thickness and friction of the piston ring. Based on these models, the studies of the PRCL lubrication problem have been developed over the years. As the investigations progress, more and more factors (oil flow[13-15], gas flow[16,17], lubrication mode[18], movement of piston rings[19], and others) are taken into count for improving the comprehensiveness of the statistical models.

Li et al. [10] developed a numerical model to study the influence of the oil supply on the lubrication performance in a two-stroke marine diesel engine. Klit et al. [9] concluded that a two-stroke engine's rings experienced three lubrication regimes (full-film, mixed, and boundary lubrication) during the operation by measuring the friction force of the PRCL with a test rig. Boundary lubrication is the lubrication regime where the interface behavior is dominated by chemical reactions that happen at the surfaces, tribofilm formation occurs, and the load is carried by the asperities[11]. A wide range of studies regarding many aspects of tribofilm formation and removal and their influence on friction and lubrication have been proposed[12,13]. In the growth of tribofilm, the asperities contact pressure plays a decisive role.

Therefore, the accurate description of asperities contact pressure is essential for analyzing the tribofilm in the PRCL system. The Stribeck curve could objectively evaluate the lubrication regime transition. This study found that when the Greenwood-Williamson model is used to build the lubrication model of a two-stroke engine, the

boundary lubrication regime could not correctly be reflected under the perspective of the Stribeck curve. Therefore, this paper can improve this situation by introducing the friction calculation model under boundary lubrication proposed by Wen into the original G-W model, which plays a vital role in the subsequent boundary lubrication and tribofilm researches of the PRCL system in two-stroke engines.

2. Numerical model description

According to previous research[14], it is known that the effect of groove pressure (the gas pressure of ring groove) on lubrication performance, which is related to the asperities contact pressure, should be attended in the numerical models. In this study, the combined statistical model for the PRCL system of a two-stroke engine consists of two numerical models: (a) the blow-by model for groove pressure, the result would be applied to the boundary condition for the oil film pressure; (b) the tribology model to predict the lubrication performance based on the improved Greenwood-Williamson model. The above two models are coupled by the radial balance force equation of the piston ring. Furthermore, as shown in Figure 1, the lubricant oil is shroud the inner liner surface with the help of injectors, rather than splashed by the crankshaft. Thus, during the operation of two-stroke engines, it is reasonable to conclude that the ring-liner contact is working on fully flooded with the lubricant oil. Two-stroke engines do not have a crosshead, so there is no secondary motion of the piston. Besides, for applying the line contact concept to the piston ring of two-stroke engines, it is essential to assume the piston ring is homogeneous in the circumferential direction. Meanwhile, the assumption makes only a small section of the ring need be taken into count, as shown in Figure 2.

In the low-speed two-stroke marine engines, the bore structure size is long, and the contact area between the ring and the liner is large, for simplification, the localized deformation on the contact interface is not considered in this paper. The study focuses on hydrodynamic lubrication. Furthermore, it is known that the temperature would have an essential impact on the viscosity and pressure of oil, gas flow, and lubrication

performance[40-41]. The impact of cavitation on the PRCL system is not considered in this paper, because the crank speed is low in the two-stroke marine engines. However, to focus on the influence of the contact model on the PRCL system, the impact of the temperature field, the cavitation, and the viscosity of oil would be considered in the next researches.

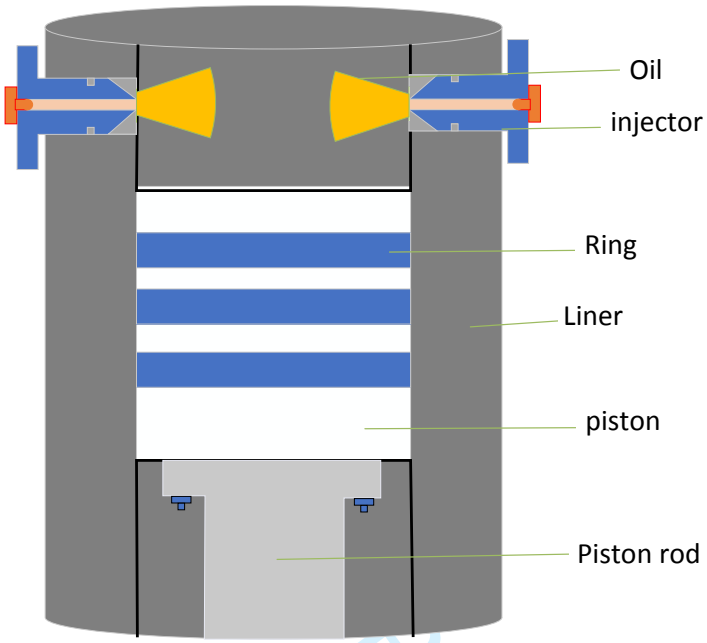

Fig.1 The scheme of oil supply of a two-stroke engine

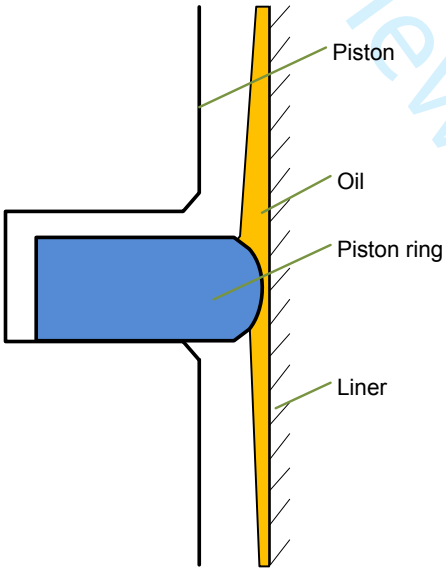

Fig.2 The scheme of the PRCL system of a two-stroke engine

Based on the concept mentioned above, the following assumptions could be applied to the numerical lubrication model of this study.

a. The lubricant is Newtonian.

b. The oil film pressure is constant across the film.

c. The temperature of the PRCL system is constant during the operation.

2.1 Blow-by model

The characteristics and structure size of two-stroke engines prompt the difference of the groove pressure analysis between four-stroke engines and them. In the blow-by studies of four-stroke engines[21-23], the groove pressure of the first ring usually is instead by the cylinder pressure, since the gap between the ring and the upper surface of the ring groove is so small that the mass of leaked gas (from the combustion chamber to groove) could be ignored. However, according to the reference[24], it is noticed that the groove pressure would be quite different from the cylinder pressure under some structure sizes of two-stroke engines.

Therefore, for a more accurate boundary condition of P the oil film pressure, this blow-by model for groove pressure would be attached to the lubrication model of a two-stroke engine. The calculation of this additional model for groove pressure could be considered an extension of the existing theoretical concept of the gas flow in the PRCL system, as shown in Figure 3.

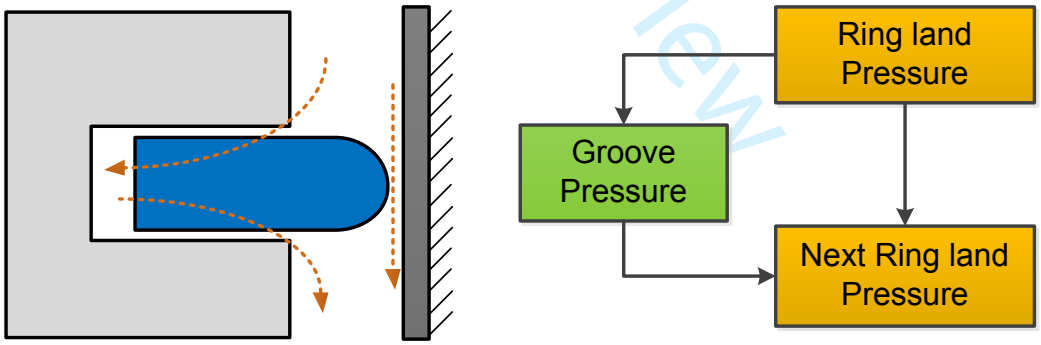

Fig.3 The scheme of the groove pressure model

The numerical description of this additional model is shown as follows, which includes the mass flow rate, the leakage area, and the gas mass balance equation of the blow-by for the ring groove.

$$dm_{groove} = \sum m_{in} - \sum m_{out} \quad (1)$$

Where dm_{groove} is the increase or decrease of gas mass in the groove, m_{in} is the gas

mass entering the groove, m_{out} is the gas mass of outing from the groove.

The following equation group obtains the gas mass flow rate through the gap between the groove and the ring[42-44].

$$\dot{Q}=\frac{dm}{dt}=\begin{cases} K_c A_n \sqrt{\frac{2k}{R_g(k-1)T_{out}}} p_{in} \left(\frac{p_{out}}{p_{in}}\right)^{\frac{1}{k}} \sqrt{1-\left(\frac{p_{out}}{p_{in}}\right)^{\frac{k-1}{k}}}, \frac{p_{in}}{p_{out}} > \left(\frac{2}{k+1}\right)^{\frac{k}{k-1}} \\ K_c A_n \sqrt{\frac{2k}{R_g(k-1)T_{out}}} p_{in} \times 0.227, \frac{p_{in}}{p_{out}} \le \left(\frac{2}{k+1}\right)^{\frac{k}{k-1}} \end{cases} \quad (2)$$

Where Q is the gas mass flow rate, P_{out} is the pressure of the outlet, P_{in} is the pressure of the inlet, A_n is the leakage area of the gap, K_c is the flow factor of leakage path, K is the heat ratio, T is the temperature of the gas chamber, R_g is the ideal gas pressure constant.

Substituting Formula (1) into Formula (2) and then, according to the following Formula (3), the groove pressure could be obtained[42-44].

$$\frac{dP}{dt}V = R_g T \frac{dm}{dt} + R_g m \frac{dT}{dt} \quad (3)$$

2.2 Average Reynolds equation

The average Reynolds equation[5] is set as the governing equation in this work, shown as Formula (4).

$$\frac{\partial}{\partial y}\left(\phi_y \frac{\rho h^3}{\mu}\frac{\partial \overline{p}}{\partial y}\right) = 6U\rho\phi_c \frac{\partial h}{\partial y} + 6U\sigma_{com}\frac{\partial(\rho\phi_s)}{\partial y} + 12\rho\phi_c \frac{\partial h}{\partial t} \quad (4)$$

Where y is the axial direction of the piston ring, p is oil film pressure, h is nominal oil film thickness, μ is the oil viscosity, U is the axial speed of piston ring, Φ_y is the pressure-flow factor, Φ_s is the shear flow factor, Φ_c is the contact factor, σ_{com} is comprehensive surface roughness[10].

$$\sigma_{com} = \sqrt{\sigma_1^2 + \sigma_2^2} \quad (5)$$

Where σ_1 is the roughness of the piston ring, σ_2 is the roughness of the liner.

Φ_y presents the pressure caused by the oil flow in the y-direction of the piston ring, which Patir and Cheng develop. In particular, for simplification of models in this study,

the engine surfaces are Gaussian distribution. The flow factors are different on Gaussian and non-Gaussian distribution surfaces[37]. The works could supply essential information about the flow factors on non-Gaussian surfaces[38-39].

The details of Formula (6) could be found in references [6] and [20].

$$\phi_y = \begin{cases} 1 - Ce^{-\gamma H}, \gamma \le 1 \\ 1 + CH^{-\gamma}, \gamma > 1 \end{cases} \tag{6}$$

Φ_s reveals additional flow generation due to the relative sliding motion of two rough surfaces [6, 20].

$$\phi_s = v_{r1}\varphi_s(H) - v_{r2}\varphi_s(H) \tag{7}$$

$$v_{r1} = (\frac{\sigma_1}{\sigma_{com}})^2, v_{r2} = (\frac{\sigma_2}{\sigma_{com}})^2 \tag{8}$$

$$\varphi_s(H) = \begin{cases} 1.899H^{0.98}\exp(-0.92H + 0.05H^2), H \le 5 \\ 1.126\exp(-0.25H), H > 5 \end{cases} \tag{9}$$

Where H is the oil film thickness ratio as shown as follows.

$$H = \frac{h}{\sigma_{com}} \tag{10}$$

Φ_c was introduced into the average Reynolds equation by Chengwei. Wang and Zheng [33] in 1989 to solve the partial film lubrication regime (H<3) in which h_T would not equal to h. In their study, by a careful analysis of the asperity deformation, it can be found that the nominal film thickness is only a function of h. Then, define $\partial\overline{h_T}/\partial h$ as the contact factor, as shown as follows.

$$\frac{\partial\overline{h_T}}{\partial x} = \frac{\partial\overline{h_T}}{\partial h}\frac{\partial h}{\partial x} = \phi_c\frac{\partial h}{\partial x} \tag{11}$$

A numerical analysis of the contact factor has been proposed [33], and its result is shown as follows.

$$\phi_c = \int_{-H}^{\infty}\varphi(S)dS \tag{12}$$

Where $\varphi(s)$ is the probability density function of standardized distribution with zero mean and unit variance, the contact area ratio is 1-Φ_c. In this study, the distribution of asperity is Gaussian Distribution.

$$\phi_c = \int_{-H}^{\infty} \varphi(s) ds = \frac{1}{2}[1 + erf(H)]$$
$$erf(H) = \int_0^H \frac{2}{\sqrt{\pi}} e^{-\xi} d\xi \quad (13)$$

Furthermore, the curve fitting formula for the contact factor is proposed in the work of Wu and Zheng,

$$\phi_c = \begin{cases} \exp(-0.6912 + 0.782H - 0.304H^2 + 0.0401H^3), 0 \le H \le 3 \\ 1, H > 3 \end{cases} \quad (14)$$

It is noticed that, in the study of the original work of Wu and Zheng, the limitation of the film thickness ratio H could be applied to the region where it is smaller than 1.0 (H<1.0).

As mentioned above, the contact model (various flow factors) attached to the lubrication model is constructed by an essential parameter, H the thickness ratio. Moreover, the value of which is decided by nominal oil film thickness, shown as the following Formula (15).

$$h = h_{\min} + h_x \quad (15)$$

Where h_x is geometric thickness between the piston ring and liner, h_{min} is minimum oil film thickness between piston ring and liner. Figure 4 illustrates the relationship between h_{min} the minimum oil film thickness and the profile of the ring.

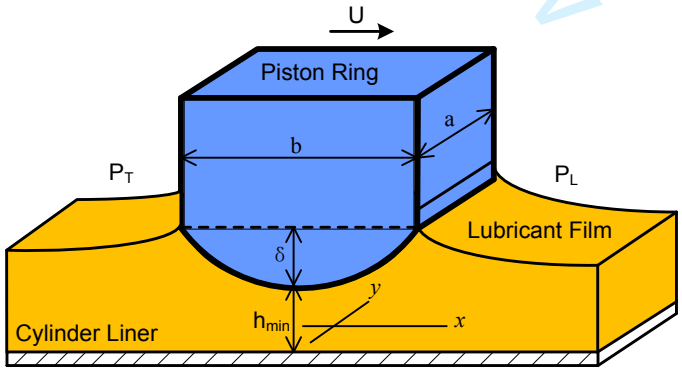

Fig.4 The scheme between the ring and the liner

It is known that any curve could be described by multiple expansion or piecewise function mathematically. In this study, the profile of the ring is assumed as barrel shape, which is expressed by a quadratic parabola, as shown in Figure 5.

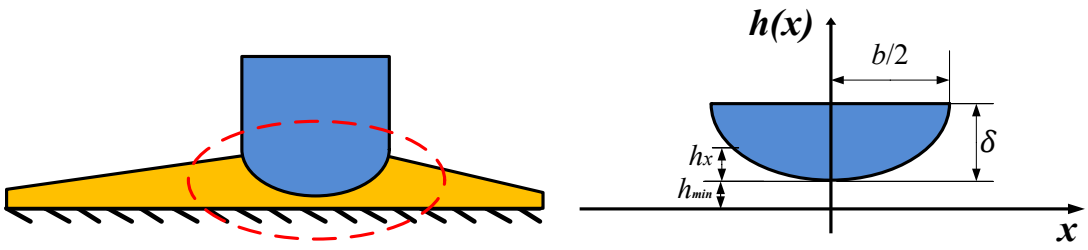

Fig.5 The mathematical description of the profile of the piston ring

According to Figure 5, it could be concluded that the oil film thickness equation, as shown as follows.

$$h = h_{\min} + \frac{\delta}{(b/2)^2} x^2 \tag{16}$$

Substituting Formula (5) to (16) into the average Reynolds equation and assuming the value of h_{min} the minimum oil film thickness, then the governing equation could be solved and obtain a P oil film pressure which could not be sure its correctness. Moreover, the correctness of P in this study could be verified by the load balance equation of the piston ring.

2.3 Load balance equation

The forces on the piston ring in the radial direction are shown in Figure 6.

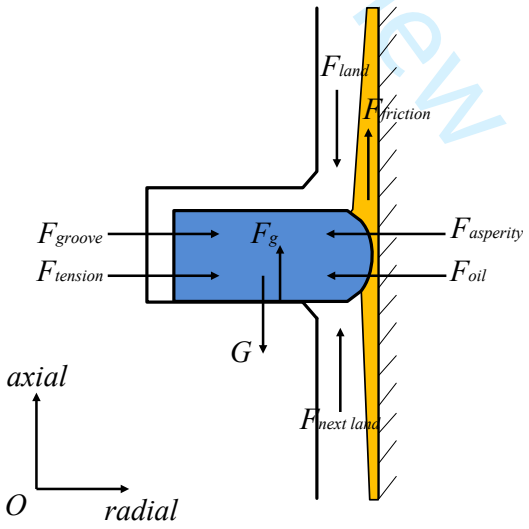

Fig.6 The forces on piston ring at the radial direction

Where F_{groove} is the groove pressure on the ring, $F_{tension}$ is the tension of the ring, F_{oil} is oil film pressure on the ring, $F_{asperity}$ is the asperity contact force on piston ring,

F_{land} is the ring land pressure (cylinder pressure), F_g is the support force on the ring by groove, $F_{next,land}$ is the next ring land pressure.

In this work, the piston ring would keep stable by the forces in the radial direction. The radial balance equation is shown as follows.

$$M_r a_r = F_{groove} + F_{tension} - F_{oil} - F_{asperity} \tag{17}$$

According to the theory, the correct P oil film pressure should satisfy the radial load balance equation as mentioned above. Thus, a computational iteration cycle for the correct P oil film pressure could be proposed, as shown in Figure 7. The convergence criteria of the load balance equation are shown as follows.

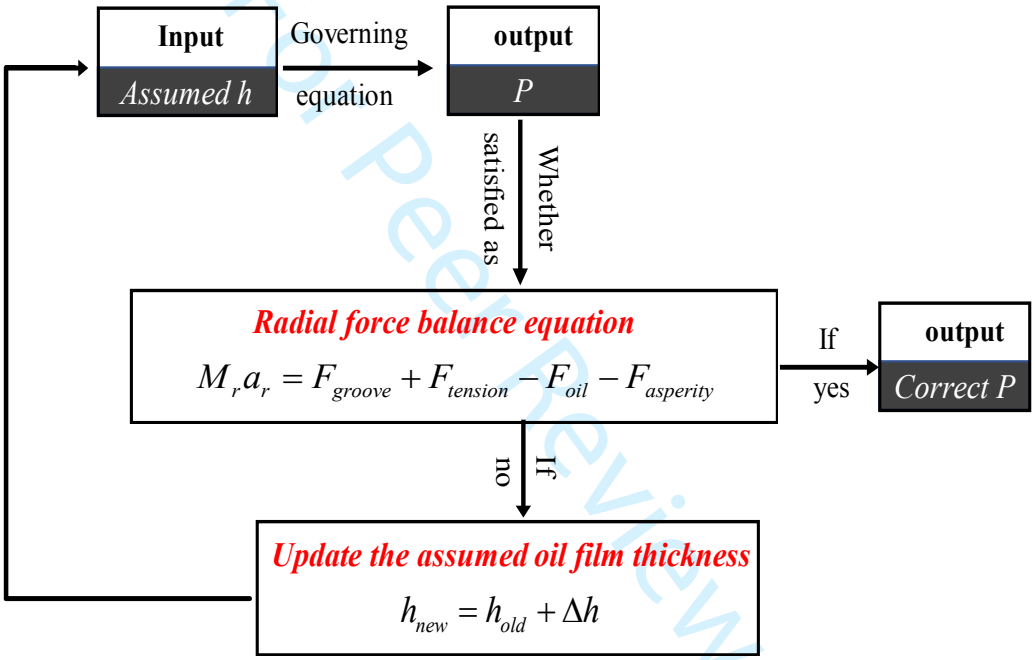

Fig.7 The computation cycle for the oil film pressure

$$\frac{F_{groove} + F_{tension} - F_{oil} - F_{asperity}}{F_{groove} + F_{tension}} < eps$$

Where *eps* is the convergence accuracy, set as 1.0×10^{-5}.

As shown in the above flow chart, it is concluded that F_{groove} the groove pressure has a significant influence on the accuracy of Foil the oil film pressure. Therefore, there should be a requirement for the precise groove pressure in the computation cycle.

2.4 Contact model

It is known that friction plays an essential role in the studies of lubrication and

tribology. The total friction includes the viscous friction of the oil $F_{f,oil}$, and the asperity contact force $F_{f,asp}$, as shown as Formulas (18)- (23).

$$F_f = F_{f,oil} + F_{f,asp} \tag{18}$$

$$F_{f,oil} = l_r \int \tau dy \tag{19}$$

$$\tau = \frac{\mu U}{h}(\phi_f + \phi_{fs}) + \phi_{fp}\frac{h}{2}\frac{\partial p}{\partial y} \tag{20}$$

$$F_{f,asp} = \mu_f F_{c,asp} + \tau_0 A_c \tag{21}$$

$$A_c = \pi^2(\varepsilon\beta\sigma)^2 A F_2(\mathrm{H}) \tag{22}$$

$$F_{c,asp} = l_r \int p_{asp} dy \tag{23}$$

Where τ_0 is the shear stress constant, l_r is the length of the ring, Φ_f, Φ_{fs}, and Φ_{fp} are the average shear factors, P_{asp} is the contact pressure, A is the nominal contact area, the details of which could be found in the reference [6] and [20], μ_f is the friction coefficient of asperities, set as 0.08 in this paper.

The contact pressure P_{asp} could be known from the Greenwood-Williamson model, which is widely used for mixed lubrication.

$$p_{asp} = \frac{16\sqrt{2}}{15}\pi(\varepsilon\beta\sigma)^2 E'\sqrt{\frac{\sigma}{\beta}}F_{5/2}(\mathrm{H}) \tag{24}$$

Where ε is the density of the asperities, β is the radius of the asperities, E' is the composite elastic modulus, which could be given by the following Formula (25).

$$\frac{1}{E'} = \frac{1\text{-}\nu_1^2}{E_1} + \frac{1\text{-}\nu_2^2}{E_2} \tag{25}$$

Where v_1, v_2, and E_1, E_2 are the Poisson's ratios and elastic moduli of the ring and the liner.

The friction coefficient Coe_f could be known as follows.

$$Coe_f = \frac{F_f}{F_{tension} + F_{groove} - M_r a_r} \tag{26}$$

There would be a likely boundary lubrication regime in the working conditions of two-stroke engines due to the harsh load and low speed near the top dead center.

Therefore, in this study, the friction coefficient proposed by Wen and Huang[31] is introduced into this contact model.

The load on the surface under boundary lubrication:

$$W=A[\alpha_w p_0+(1-\alpha_w)p_L] \tag{27}$$

Where α_w is the percentage of solid contact area in the real contact area A, p_0 is the plastic flow pressure, p_l is the lubricant oil pressure. For boundary lubrication, the value of α_w is usually below 0.01 or 0.001 or even smaller. Thus, Formula (27) could be simplified to the following Formula (28).

$$W=Ap_L \tag{28}$$

The friction coefficient under boundary lubrication:

$$f_{BL}=\frac{\tau_L}{\overline{p}}+f_p \tag{29}$$

The concerned parameters can be found in reference [31]. The improved contact model in this study, which could be applied to all lubrication regimes, could be proposed, as shown in Figure 8.

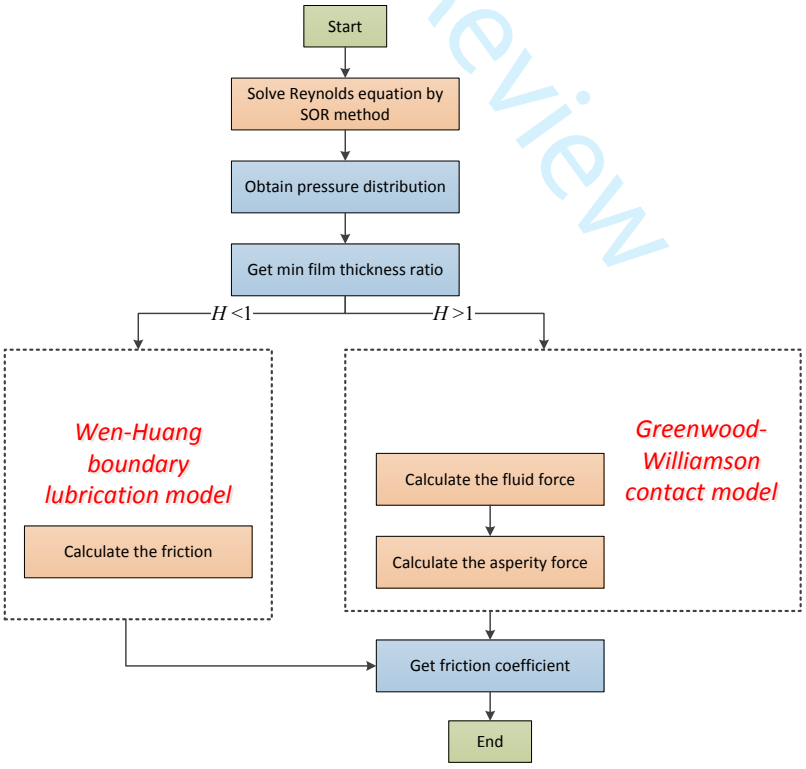

Fig.8 The calculation flow chart for two-stroke engines

3. The model validation

3.1 Model validation with reference

This program requires many detailed parameters of a low-speed two-stroke engine, but the currently existing reference does not meet this demand. Therefore, a four-stroke engine whose structure is closer to a two-stroke engine has been chosen for verification. With the help of Formulas (1) – (26), the friction force could be presented. The friction coefficient from the above model is verified against the results of reference [27]. The input parameters and cylinder pressure are shown in Table 1 and Figure 9, respectively. The friction force results of the comparison with the reference are shown in Figure 10.

Table 1. The input parameters

Parameter	Value	Unit
Speed	1500	r/min
Stroke	0.23	m
Length of the connecting rod	0.473	m
The diameter of the cylinder bore	230	mm
The surface roughness of the cylinder	0.001	mm
The surface roughness of the ring	0.0008	mm
The tension of the top ring	150	kPa

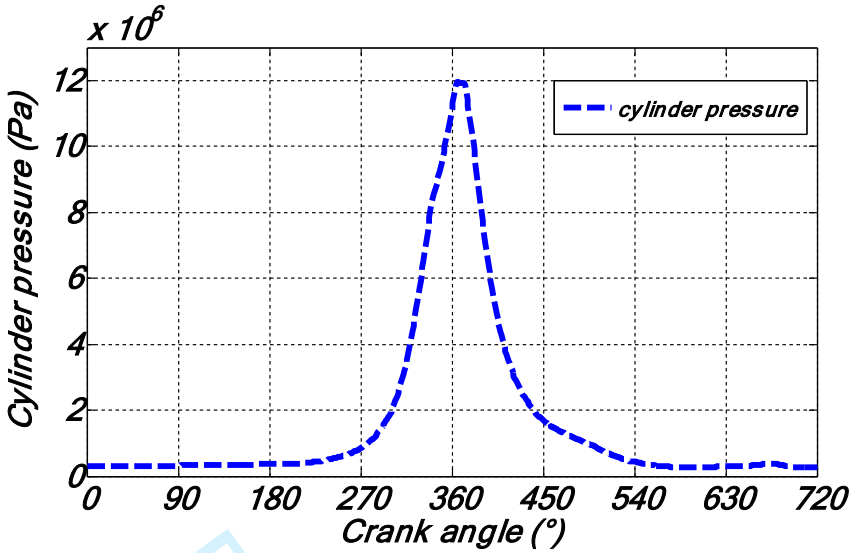

Fig.9 The cylinder pressure of the reference [27]

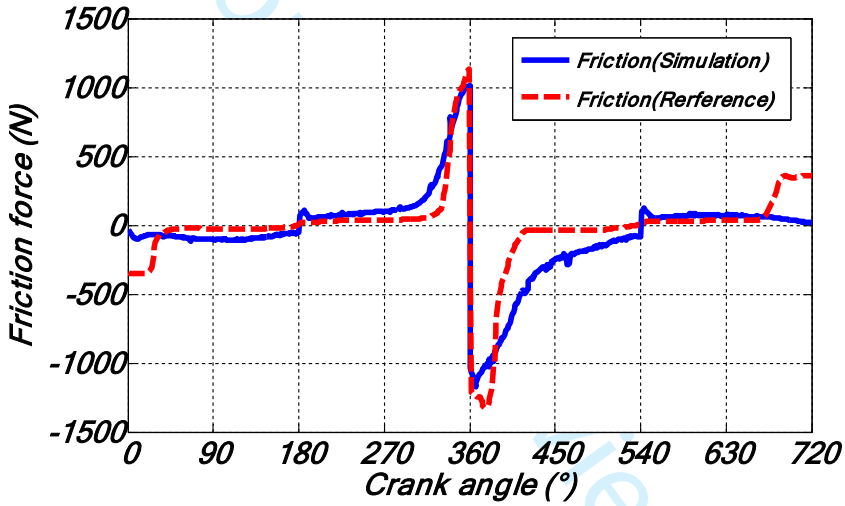

Fig.10 The friction force

It is shown that the predictions of oil film thickness and the friction force in the model of this study agree well with the reference [27]. Although, in the crank angle regime of 360°-540°, the reference and the simulation value is different since this regime is the power stroke that results in the groove pressure that would significantly influence the lubrication model. The differences between the results of reference [27] and the simulation of this study are caused by the method to deal with the contact model and groove pressure, which are essential parts of the radial forces balance equation for the lubrication model. The groove chamber (as shown in Fig.3) plays the role of temporarily storing high-pressure gas during the cylinder pressure explosion regime. This would cause the pressure output to have a delay, so that the friction in Figure 10

would decrease relatively slowly when near the top dead center (TDC).

3.2 The comparison of results

The mentioned above model, combined with the contact model proposed by Wen and the Greenwood-Williamson model, is applied to the first piston ring of a two-stroke engine. There are some details about the engine listed in Table 2 and the cylinder pressure shown in Figure 11.

Table 2. The parameters of the two-stroke engine

Parameter	Value	Unit
Maximum cylinder pressure	220.00	Bar
Crank radius	0.80	m
Power for single liner	920.00	kW
Oil viscosity	0.08	Pa·s
Piston ring roughness (Rq)	0.80	mm

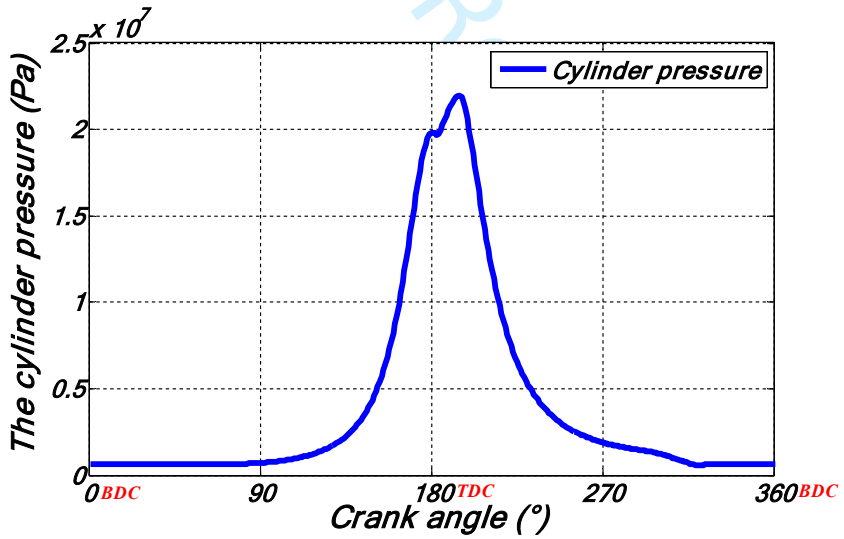

Fig.11 The cylinder pressure of the engine

The frictions calculated by different models are shown in following Figure 12(a). The coefficients of friction could be obtained by Formula (26), as shown in Figure 12(b).

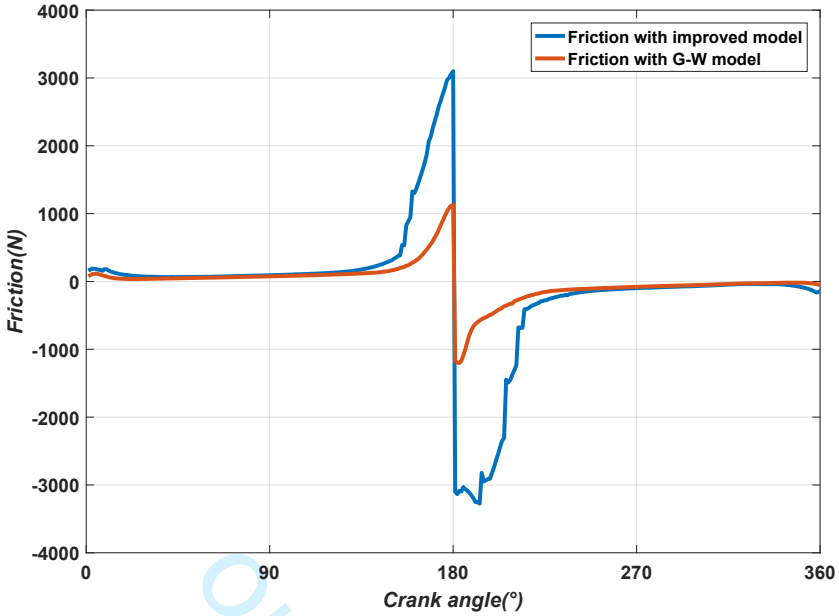

(a) The frictions with different models

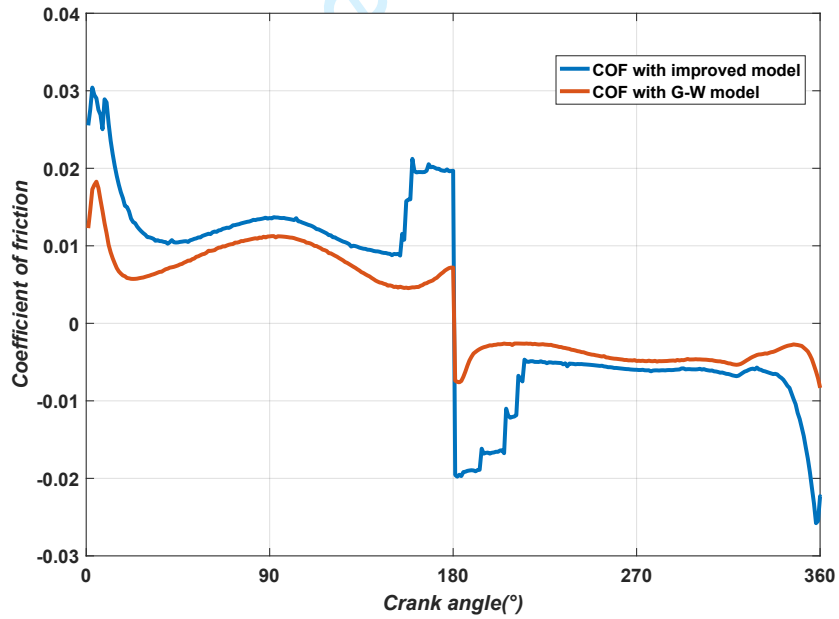

(b) The coefficients of friction with different models

Fig.12 The calculation results by improved model and G-W model

It is known that under boundary lubrication, friction at the contact interface would increase. In both of these above results, there has been an increase in friction at TDC. With the improved model, there are some discontinuous intervals in the friction and the coefficient, which are caused by the judgment of boundary lubrication conditions in this model. At the boundary lubrication regime, the gap between the contact surfaces is

reduced, the interaction of the rough peaks is strengthened, and the oil film thickness is reduced to the thickness of one or two monolayers. The tribology performance is completely determined by the physical and chemical effects of the film and the contact mechanics of rough peaks. Simultaneously, in the boundary lubrication regime, the surface load is considered to have reached the limit [31]. Therefore, the ultimate shear stress is used in the model. However, the lubrication regimes could not be distinguished directly in Figure 12. By referring to the concept, the lubrication regime could be distinguished by thickness ratio H. It could be concluded that the full-film lubrication dominates when $H>3$, and the mixed lubrication happens in the case of $1<H<3$, and the boundary lubrication controls at the part of $H<1$[34].

Therefore, thickness ratio H would be introduced in both results above, as shown in Figure 13. In this way, with the help of H, this curve, which could take advantage of the crank angle to distinguish the lubrication regimes, could be applied to the engineering industries.

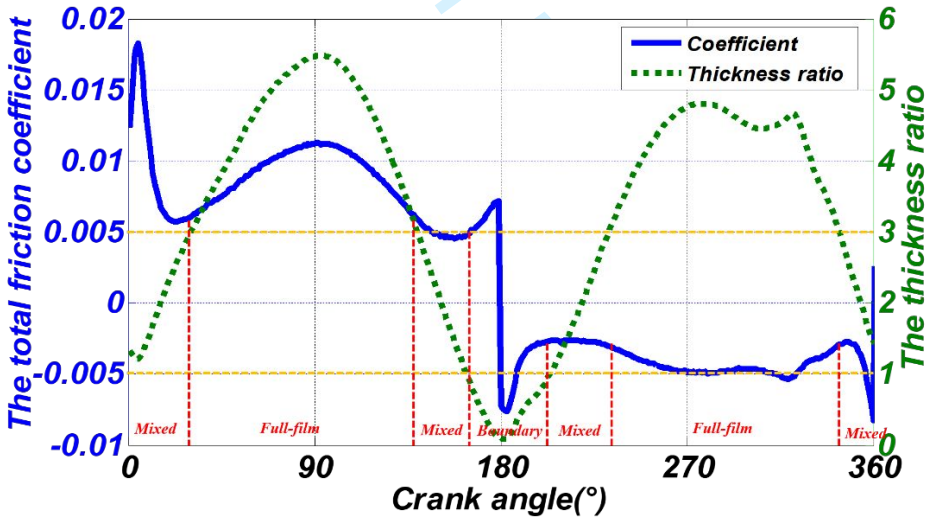

(a) The lubrication regime transition with the G-W model

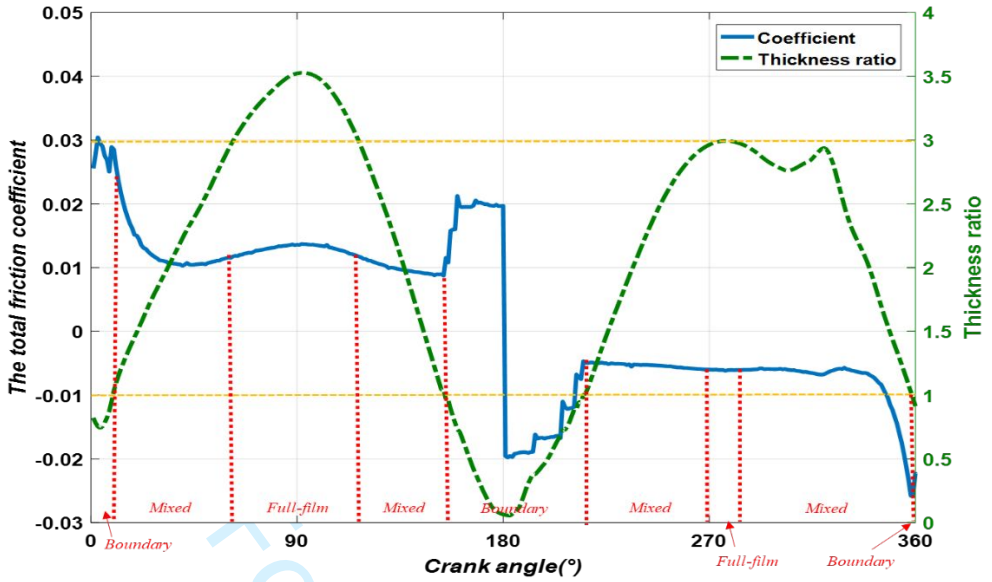

(b) The lubrication regimes transition with the improved model

Fig.13 The lubrication regime transition curves based on different contact models

In Figure 13, the lubrication regimes could be directly distinguished from these two figures. However, due to the introduction of the boundary lubrication module proposed by Wen, the lubrication regime transition law has been changed. Besides, Figure 13 could be efficient for engine industries to monitor the performance of ICEs under work conditions and improve the corresponding data (structure, lubrication oil, and surface parameters) by refer to this figure.

Notably, in the cases of this work, there is some strange phenomenon in Figure 13:

(1) There is a fluctuation during the crank angle of 320° to 340° in the thickness ratio in both cases above. The same fluctuation during the power stroke in the cylinder pressure (shown in Figure 11) results in this phenomenon in the ratio and COF of Figure 13.

(2) In compression and suction stroke (near 0° and 360°), the coefficients are significant than that of the power and exhaust stroke (near 180°) in both cases. The friction coefficient is equal to the friction divided by the load (the sum of the tension of the ring and the groove pressure). In this stroke, the friction is slight, but the groove pressure is even smaller than the other stroke. Meanwhile, reference [26] proposed that

the coefficients near TDC are also smaller than the others. Therefore, this phenomenon is reasonable.)

(3) The boundary lubrication would happen at TDC (near 180°). However, in this G-W model regime, the COF is smaller than that of full-film lubrication. As mentioned above, the friction of the boundary lubrication regime is significant (as shown in Figure 13), but the influence of groove pressure on reducing COF is even more significant. On the contrary, in the boundary lubrication regime, the COF has a gentler trend and a more significant value. From the perspective of the Stribeck curve, the COF under boundary lubrication is in a limit state. The value does not change.

In summary, although Figure 13 could distinguish the lubrication regime directly. There is no doubt that the abscissa doped with the influence on COF (the load is changed with crank angle) leads to the difficulty of verifying the lubrication regime transition in the mechanism viewpoint in Figure 13. Therefore, a COF image with a dimensionless abscissa must be established for objectively evaluating the lubrication regime transition for exploring the difference between these two models, which would be discussed in the following sections.

4. The Stribeck curves with the improved model and the G-W model

For the accurate description of the lubrication regime transition and the understanding of boundary lubrication in two-stroke engines, the Stribeck curve is introduced into this study. Meanwhile, the following sections would show the modified model (which introduced the Wen boundary lubrication module) improves the problem that the original model cannot reflect the boundary lubrication regime in the form of the Stribeck curve.

4.1 The process of obtaining the Stribeck curves

Since obtaining the Stribeck curve of a two-stroke engine is similar. For saving space, this paper only lists the process of obtaining the Stribeck curve of the G-W model.

Firstly, the abscissa of the Stribeck curve is Hersey number (Viscosity*Velocity/Load). Figure 14 shows the velocity and the Hersey number of the two-stroke engine, and the load has been shown in Figure 11.

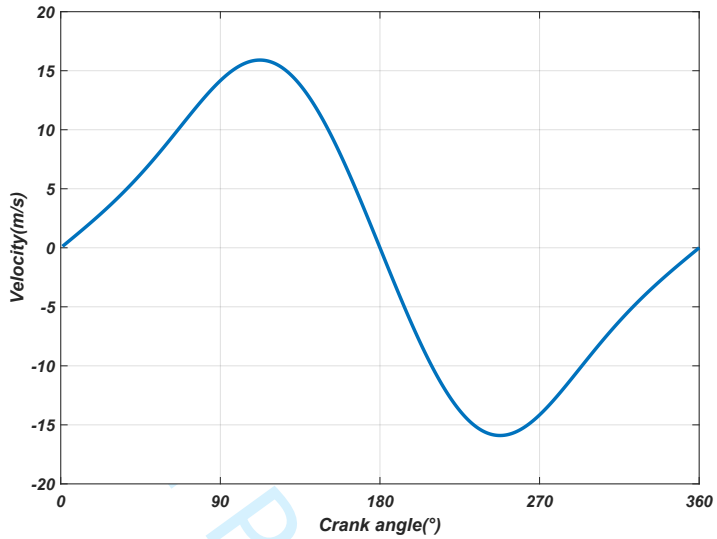

(a) The velocity of the two-stroke engine

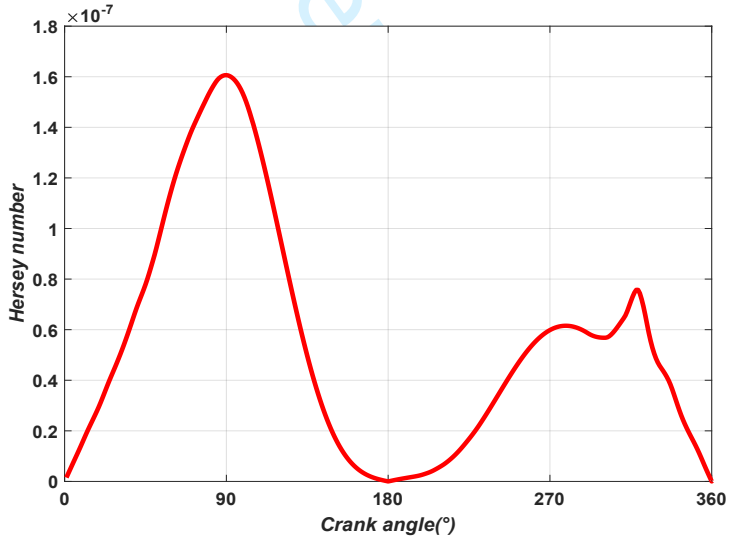

(b) The Hersey number of the two-stroke engine

Fig.14 The velocity and Hersey number

Then, the Hersey number should be rearranged from small to large, which would be the abscissa. The COF as a function of the Hersey number sorted from small to large is shown in Figure 15.

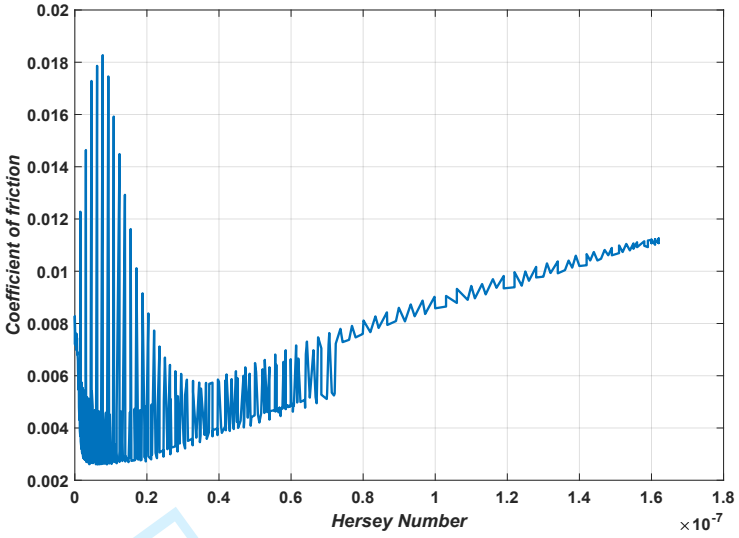

Fig.15 The friction coefficient as a function of Hersey number in total strokes

It is illustrated from Figure 15 that there is two pulses trend in each corresponding Hersey number when smaller than about 0.7×10^{-7}, which is caused by the that each Hersey number corresponds to four crank angles (shown in Figure 14.b). Thus, it could be inferred that the curve in Figure 15 consists of four Stribeck curves from four four-half-strokes (each 90 crank angles). In Figure 16, the Stribeck curves in each half stroke are shown.

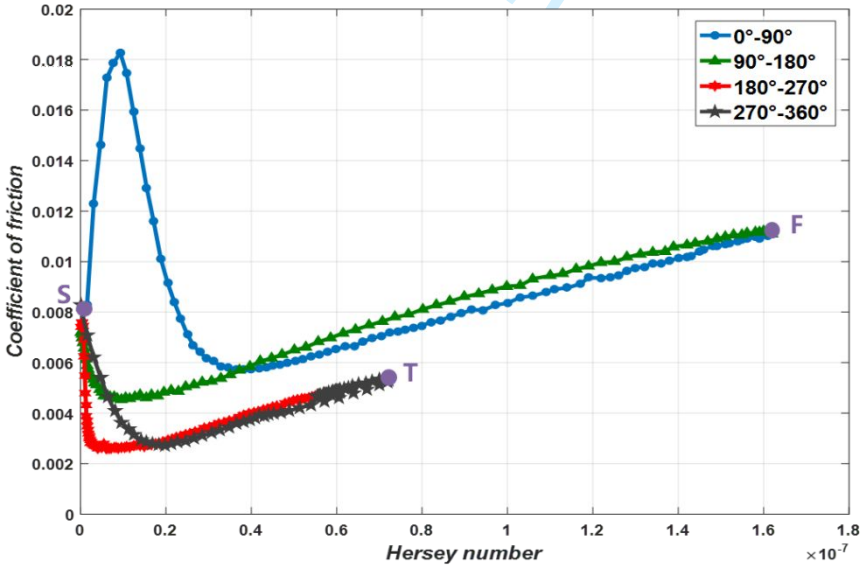

Fig.16 The Stribeck curves in each half-stroke with the G-W model

Combined with Figure 14, it could be inferred from Figure16 that the friction coefficient, which is a function of crank angles, starts from point *S* to point *F* along the

blue line in the first half stroke (0°-90°). Then the coefficient would arrive at point *S* from point *F* along the green line in the second half stroke (90°-180°), and next to the coefficient starts from point *S* to point *T* along the red line in the third half stroke (180°-270°). Finally, the coefficient would end at point *S* from point *T* along the black line in the fourth half stroke (270°-360°). It also could be known from Figure 16 that the lubrication regimes would be transferred with the friction coefficient from some modes to others.

4.2 The comparison between the Stribeck curves of both models

As mentioned above, the Stribeck curves with the G-W model and the improved model could be obtained. Furthermore, the abscissa of each Stribeck curve of both models has been converted to logarithmic form to show the lubrication regime transition process clearly, as shown in Figure 17.

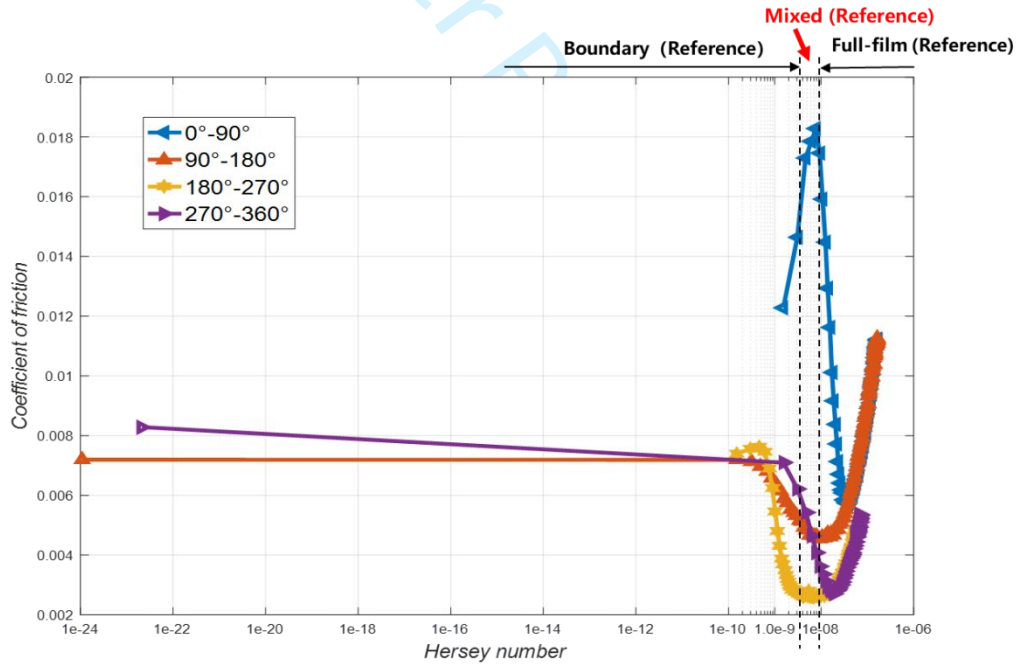

(a) The Stribeck curves with the G-W model

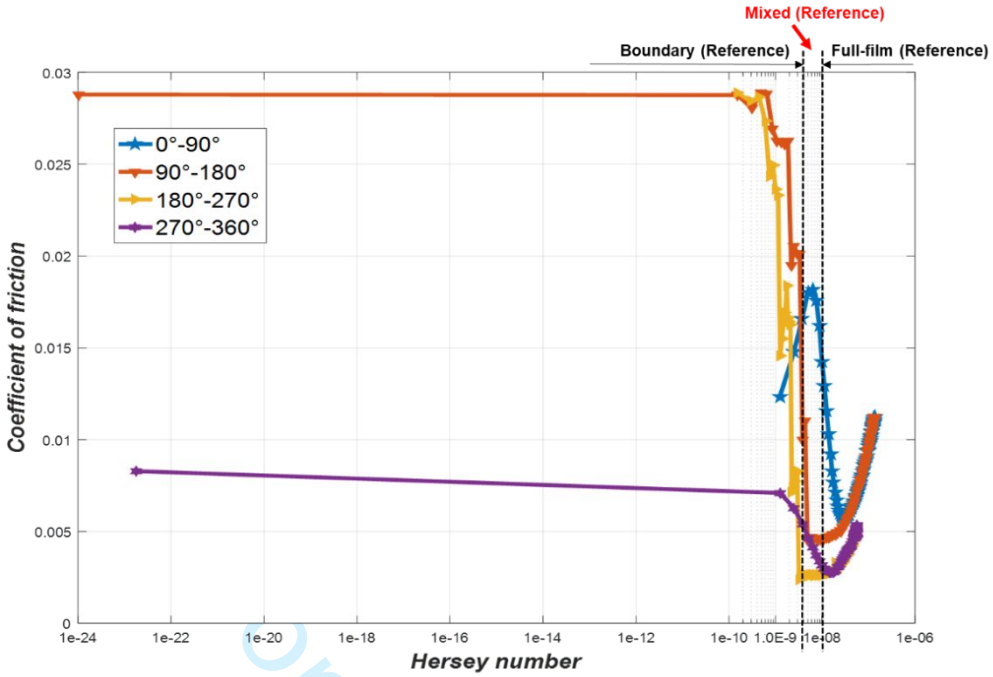

(b) The Stribeck curves with the improved model

Fig.17 The Stribeck curves in the form of logarithmic

There is some essential information that could be inferred by Figure 17:

(1) The inflection points of mixed lubrication and full-film lubrication in each curve of both models are consistent, almost the same as 10^{-8} in reference [31]. It could be concluded that the contact module of both models in this study is accurate in mixed and full-film lubrication regimes.

(2) In the 90°-180° (red line) curve of the G-W model, the COF of the full-film lubrication regime is greater than that of the mixed lubrication regime, as shown in Figure 17(a). The phenomenon does not follow the basic concepts of tribology. But the experiment results from reference [32], to a certain extent, show the reasonability of this.

However, with the improved model in this study, the COF under the boundary lubrication regime is more significant than those of other regimes. Furthermore, within error, the COF trend under boundary lubrication is at a limit, which is in line with the tribology law.

(3) According to Figure 13(a), the regime where should be boundary lubrication on the 180°-270° (yellow line) of the G-W model shows the mixed lubrication regime

in Figure 17(a). Although the 90°-180° (red line) and 270°-270° (purple line) have the boundary lubrication in Figure 17(a), there are only 1 to 2 points in this area, which could be regarded as weak points within the model accuracy error range.

However, in Figure 17(b), the modified model in this study improves this phenomenon. All the lubrication regimes, including the boundary lubrication regime, have been reflected. Therefore, it could be concluded that the improved model has a more accurate ability than that of the G-W model in predicting the boundary lubrication regime.

It is worth noting that there are some discontinuous intervals in the Stribeck curves of the improved model. Therefore, the model needs further revision and improvement. Since the load and crankshaft speed, the tribology lubrication model of two-stroke engines should introduce the boundary lubrication, the tribofilm growth module, and its influence on the ICEs cycle for making the statistic model more complete and accurate. These factors would be considered in our following researches. Furthermore, the various Stribeck's curves show the reduction of coefficient of friction to a minimum after the mixed regime, before an increasing trend. This is indicative that in future work, the localized deformation of the PRCL system should be considered.

5. Conclusion

This study firstly proves that the boundary lubrication regime does exist in two-stroke engines, as shown in Figure 13. Then, it is known that there is tribofilm growth under the boundary lubrication regime in the two-stroke engines. Furthermore, the tribofilm growth model is directly related to the asperities contact pressure [34]. Afterward, it is found that the results as shown in Figure 13 could not objectively evaluate the accuracy of coefficients under the boundary lubrication regime. Therefore, the Stribeck curve is introduced into this study because of its dimensionless abscissa. However, it is found that the classic G-W contact mode could not reflect the boundary lubrication regime precisely, as shown in Figure 17(a). Finally, the friction calculation

under the boundary lubrication, proposed by Wen, is introduced into this study to combine with the G-W contact model. The results (as shown in Figure 17) shows that this model in this study could improve the accuracy of the friction coefficients under the boundary lubrication regime. Therefore, in future work, the improved contact model could be applied to the calculation of asperities contact pressure, which would provide a more precise tribofilm growth rate. However, there are some discontinuous intervals in the friction and the coefficient of the improved contact model in this study. Therefore, the model needs further revision and improvement.

The other conclusions could be drawn from the results of this model as follows,

(1) With the influence of gas pressure, the total friction coefficient of the power stroke is different from that of the compression stroke. It is concluded that the groove pressure should be taken into count in the lubrication model of the piston ring in two-stroke engines.

(2) Mixed lubrication would happen instead of boundary lubrication at BDC, even though the speed is low, and the load decides the lubrication regime. Therefore, the lubrication modes should consider the speed and load comprehensively.

(3) By comparing Figure 13 and Figure 17, it could be known that there are two different views (engineering and lubrication mechanism) to deal with this lubrication regime transition.

a. From the engineering perspective, the lubrication regimes could be distinguished directly by crank angles in Figure 13. With the help of this curve, the optimization of work conditions or other aspects at corresponding crank angles could be proposed to improve the lubrication performance. Some researches that focus on different lubrication regimes of engines could be developed at different specific crank angles.

b. From the perspective of the lubrication mechanism, the changing trend of lubrication regimes in each half stroke by the Stribeck curves in Figure 17. Thus, based on this figure, some studies that focus on the mechanism of lubrication transition in engines could be proposed.

c. From Figure 17(a) and Figure 17(b), it could be suggested that a boundary lubrication module should be introduced into the G-W model for describing all lubrication regimes

transition in two-stroke engines.

The model in this study would be improved in future work, focusing on the tribofilm growth and tribo-chemistry reaction based on both the views mentioned above (engineering and lubrication mechanism).

6 Acknowledgements

This work is supported by the Marine Low-Speed Engine Project –Phase 1 (Grant no. **CDGC-KT0302**) in China and the Engineering and Physical Sciences Research Council (**grant number EP/001766/1**) as a part of 'Friction: The Tribology Enigma' Programme Grant (www.friction.org.uk), a collaboration between the Universities of Leeds and Sheffield in the U.K.

7 Nomenclature

dm_{groove}	=	the increase or decrease of gas mass in the groove, *Kg*
m_{in}	=	the gas mass entering the groove, *Kg*
m_{out}	=	the gas mass of outing from the groove, *Kg*
Q	=	the gas mass flow rate, *Kg/s*
P_{out}	=	the pressure of the outlet, *Pa*
P_{in}	=	the pressure of the inlet, *Pa*
A_n	=	the leakage area of the gap, m
K	=	the heat ratio
T	=	the temperature of the gas chamber, *K*
R_g	=	the ideal gas pressure constant, 8.314 *J/(mol•K)*
t	=	time, *s*
V	=	the volume of the gas chamber, m^3
y	=	the axial direction of the piston ring
p	=	oil film pressure, *Pa*
h	=	the nominal oil film thickness, *m*
μ	=	the oil viscosity, *Pa•s*
U	=	the axial speed of piston ring, *m/s*
Φ_y	=	the pressure-flow factor
Φ_s	=	the shear flow factor
Φ_c	=	the contact factor
σ_{com}	=	comprehensive surface roughness, *m*
v_r	=	the Poisson's ratio
γ	=	the rough surface direction parameter
H	=	the oil film thickness ratio
h_T	=	the average oil film thickness, *m*
h_x	=	geometric thickness between the piston ring and liner, *m*
h_{min}	=	minimum oil film thickness between the piston ring and liner, *m*
b	=	the axial height of piston ring, *m*
δ	=	the radial height of piston ring profile, *m*

F_{groove}	=	the groove pressure on the ring, N
$F_{tension}$	=	the tension of the ring, N
F_{oil}	=	the oil film pressure on the ring, N
$F_{asperity}$	=	the asperity contact force on piston ring, N
F_{land}	=	the ring land pressure (cylinder pressure) , N
F_g	=	the support force on the ring by groove, N
$F_{next,land}$	=	the next ring land pressure, N
M_r	=	the mass of ring, Kg
a_r	=	the acceleration of the piston ring in the radial direction, m/s^2
$F_{f,\,oil}$	=	the viscous friction of the oil, N
$F_{f,\,asp}$	=	the asperity contact force, N
F_f	=	the total friction, N
μ_f	=	the contact friction coefficient
τ_0	=	the shear stress constant
l_r	=	the length of the ring, m
P_{asp}	=	the contact pressure, Pa
A	=	the nominal contact area, m^2
ε	=	the density of the asperities, kg/m^3
β	=	the radius of the asperities, m
E'	=	the composite elastic modulus, Pa
Coe_f	=	the coefficient of friction
W	=	the load on the surface under boundary lubrication, N
α_w	=	the percentage of solid contact area in the real contact area
p_0	=	the plastic flow pressure, Pa
p_l	=	the lubricant oil pressure, Pa
f_{BL}	=	the friction coefficient under boundary lubrication
τ_L	=	the fluid shear strength

8 Reference

[1] Jeng, Y. Theoretical analysis of piston-ring lubrication. Part 1: fully flooded lubrication. STLE Tribology Trans., 1992, 35,696-706.

[2] Mcgeeham James A. A literature review of the effects of piston and ring friction and lubricating oil viscosity on fuel economy. SAE Trans 1978; 87: 2619-2638.

[3] Yong Li, Haijie Chen, Tian Tian. A Deterministic Model for Lubricant Transport within Complex Geometry under Sliding Contact and its Application in the Interaction between the Oil Control Ring and Rough Liner in Internal Combustion Engines, SAE 2008-01-1615.

[4] Rohde, S. M., Whitaker, K. W., and McAllister, G. T. A mixed friction model for dynamically loaded contacts with application to piston ring lubrication. In Surface

Roughness Effects in Hydrodynamic and Mixed Lubrication, Proceedings of the ASME Winter Annual Meeting, 1980, 19-50.

[5] Greenwood J. A., Tripp J. H. The contact of two nominally flat rough surfaces. Proc IMechE, 1970, 185: 625-634.

[6] Patir, N., Cheng, H. S. An average flow model for determining effects of three-dimensional roughness on partial hydrodynamic lubrication. Trans, ASME, J. Lubric. Technol, 1978,100: 12-17.

[7] Tomanik, E. et al. "A simple numerical procedure to calculate the input data of Greenwood-Williamson model of asperity contact for actual engineering surfaces." Leeds-Lyon Symposium on Tribology: Tribological research and design for engineering systems TRIBOLOGY SERIES, 41, pp. 205-216, 2003.

[8] Dowson, D., Economou, P. N., Ruddy, B. L., Strachan, P. J., Baker, A.J. Piston ring lubrication., Part Ⅱ: theoretical analysis of a single ring and complete ring pack. In Energy Conservation Through Fluid Film Lubrication Technology: Frontiers in Research and Design, Proceedings of the ASME Winter Annual Meeting, 1979, 23-52.

[9] Klit P., Volund A. Experimental piston ring tribology for marine diesel engines. In: Proceedings of STLE/ASME international joint tribology conference, Miami, FL, 20-22 October 2008, pp. 493-497. New York: ASME.

[10] Li T. Y., Ma X., Lu X., Wang, C., Jiao B., Xu H., Zou D. Lubrication analysis for the piston ring of a two-stroke marine diesel engine taking account of the oil supply. International Journal of Engine Research, 2019: 1468087419872113.

[11] Ghanbarzadeh A , Wilson M , Morina A , et al. Development of a new mechano-chemical model in boundary lubrication[J]. Tribology International, 2016:573-582.

[12] Studt P. Boundary lubrication: adsorption of oil additives on steel and ceramic surfaces and its influence on friction and wear.Tribol Int 1989;22.2:111–9.

[13] Morina A , Neville A . Tribofilms: aspects of formation, stability and removal[J]. Journal of Physics D Applied Physics, 2007, 40(18):5476.

[14] Lyu X , Azam A , Wang Y , et al. An efficient procedure to predict the dynamic loads for piston liner systems in marine engines[J]. International Journal of Engine Research, 2021.

[15] Herbst H., Priebsch H., Simulation of piston ring dynamics and their effect on oil consumption, 2000, SAE Paper, No.2000-21-0919.

[16] Koszalka G., Application of the piston-rings-cylinder kit model in the evaluation of operational changes in blowby flow rate, 2010, Maintenance and Reliability, 48: 72-81.

[17] Ruddy B., Dowson D., Economous P. N., The prediction of gas pressure within the ring packs of large bore diesel engines, 1981, Journal of Mechanical Engineering Science, 23: 295-304.

[18] Bolander N. W., Barber G. C., The effect of roughness on piston ring lubrication, 2007, Tribology Transactions, 50: 248-256.

[19] Wolff A., Simulation based study of the system piston–ring–cylinder of a marine two-stroke engine, 2014, Tribology Transactions, 57: 653-667.

[20] Patir N., Cheng H. S., Application of average flow model to lubrication between rough sliding surfaces, 1979, Transactions of the ASME, 101: 220-229.

[21] Tian, Tian. Modeling the performance of the piston ring-pack in internal combustion engines. Diss. Massachusetts Institute of Technology, 1997.

[22] Han D. C., Lee J. S., Analysis of the piston ring lubrication with a new boundary condition, 1998, Tribology international, 31(12): 753-760.

[23] Ma M. T., Sherrington I., Smith E. H., et al., Development of a detailed model for piston-ring lubrication in IC engines with circular and non-circular cylinder bores, 1997, Tribology International, 30(11): 779-788.

[24] Lv X. Y., Lu X. Q., Ma X., Distribution and influence on lubrication performance of gas pressure in groove of piston ring pack, 2019, CIMAC Congress, No. 384.

[25] Stribeck R., Die Wesentlichen Eigenschaften der Gleit und Rollenglager, Z. Ver. Dtsch, 1902, Ing., 36:1341-1348.

[26] Bolander, N. W., et al. Lubrication regime transitions at the piston ring-cylinder liner interface. Proceedings of the Institution of Mechanical Engineers, Part J: Journal of Engineering Tribology 219.1 (2005): 19-31.

[27] Guo, Yibin, et al. A mixed-lubrication model considering elastoplastic contact for a piston ring and application to a ring pack. Proceedings of the Institution of Mechanical

Engineers, Part D: Journal of Automobile Engineering 229.2 (2015): 174-188.

[28] Wu, C. W., and L. Q. Zheng. An average Reynolds equation lubrication with a contact factor for partial film. Journal of Tribology 111.1 (1989): 188-191.

[29] Greenwood, James A., and J. H. Tripp. The contact of two nominally flat rough surfaces. Proceedings of the institution of mechanical engineers 185.1 (1970): 625-633.

[30] Patir, Nadir, and H. S. Cheng. Application of average flow model to lubrication between rough sliding surfaces. (1979): 220-229.

[31] Wen S, Huang P. Principles of Tribology [J]. Journal of Tribology, 1977, 99(2):305-306.

[32] Hakan, Adatepe, and, et al. An experimental investigation on friction behavior of statically loaded micro-grooved journal bearing[J]. Tribology International, 2011.

[33] Wu, C. W., and Zheng, L. Q. An average Reynolds equation for partial film lubrication with a contact factor. ASME J.Tribology, 1989,(111):188-191

[34] Akchurin A , Rob Bosman. A Deterministic Stress-Activated Model for Tribo-Film Growth and Wear Simulation[J]. Tribology Letters, 2017, 65(2):59.

[35] Leighton M , Morris N , Gore M , et al. Boundary interactions of rough non-Gaussian surfaces[J]. Proceedings of the Institution of Mechanical Engineers Part J Journal of Engineering Tribology 1994-1996 (vols 208-210), 2016:1350650116656967.

[36] Pei J , X Han, Y Tao, et al. Mixed elastohydrodynamic lubrication analysis of line contact with Non-Gaussian surface roughness[J]. Tribology International, 2020, 151:106449.

[37] Kim T W , Cho Y J . The Flow Factors Considering the Elastic Deformation for the Rough Surface with a Non-Gaussian Height Distribution[J]. Tribology Transactions, 2008, 51(4):542-542.

[38] Gu C , X Meng, Wang S , et al. Research on Mixed Lubrication Problems of the Non-Gaussian Rough Textured Surface With the Influence of Stochastic Roughness in Consideration[J]. Journal of Tribology, 2019, 141(12):1-36.

[39] Leighton M , Rahmani R , Rahnejat H . Surface-specific flow factors for prediction of friction of cross-hatched surfaces[J]. Surface Topography Metrology & Properties, 2016, 4(2):025002.

[40] Ishijima T , Shimada A , Harigaya Y , et al. An Analysis of Ring Temperature, Oil Film Temperature, Oil Film Thickness and Heat Transfer on a Piston Ring of an IC Engine in Consideration of Ring Movement in a Cycle[C]. Asme Internal Combustion Engine Division Spring Technical Conference. 2006:665-676.

[41] Dolatabadi N , Forder M , Morris N , et al. Influence of advanced cylinder coatings on vehicular fuel economy and emissions in piston compression ring conjunction[J]. Applied Energy, 2020, 259.

[42] Keribar R , Dursunkaya Z , Flemming M F . An Integrated Model of Ring Pack Performance[J]. Journal of Engineering for Gas Turbines & Power, 1991, 113(3):382-389.

[43] Wannatong K , Chanchaona S , Sanitjai S . Simulation algorithm for piston ring dynamics.[J]. Simulation Modelling Practice and Theory, 2008, 16(1):127-146.

[44] SHAPIRO, Ascher H . The dynamics and thermodynamics of compressible fluid flow[M]. Ronald Press Co, 1954.